



An efficient Vlasov-Poisson solver & deep parametric analysis of cylindrical emissive probes

Sadaf Shahsavani, Xin Chen, G. Sánchez-Arriaga

Universidad Carlos III de Madrid, Spain

APS-DPP 2020, 9-13 November

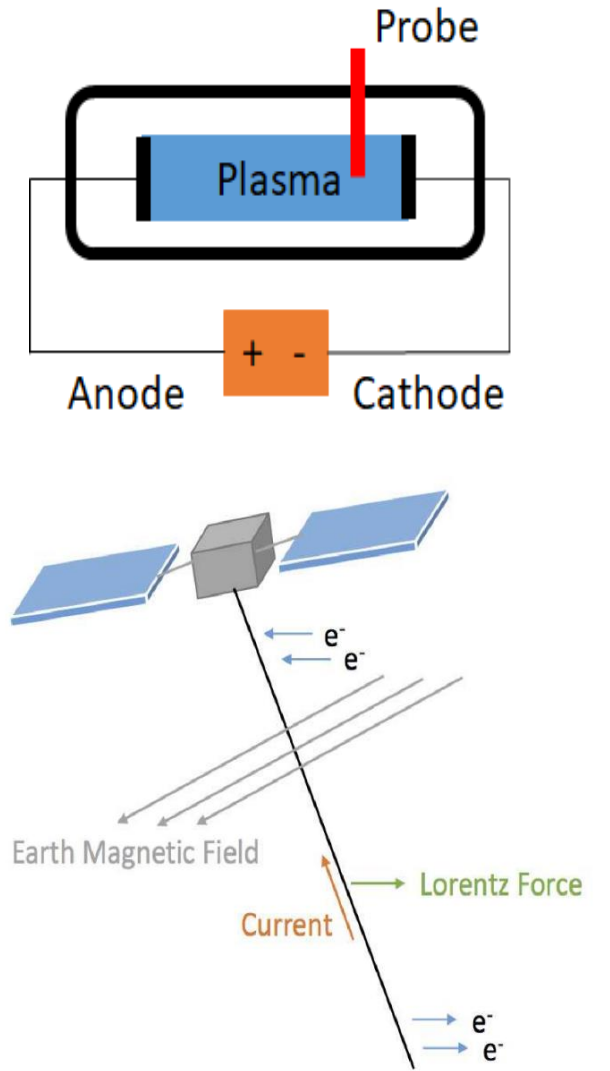
Index

- Introduction
- IV Curve Database
- Numerical Results
- Conclusions and Future work

Introduction

Introduction

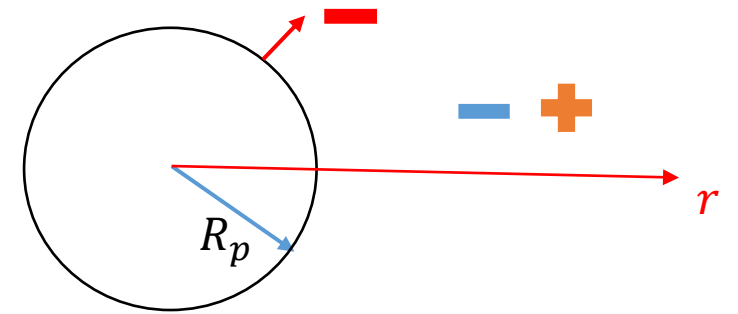
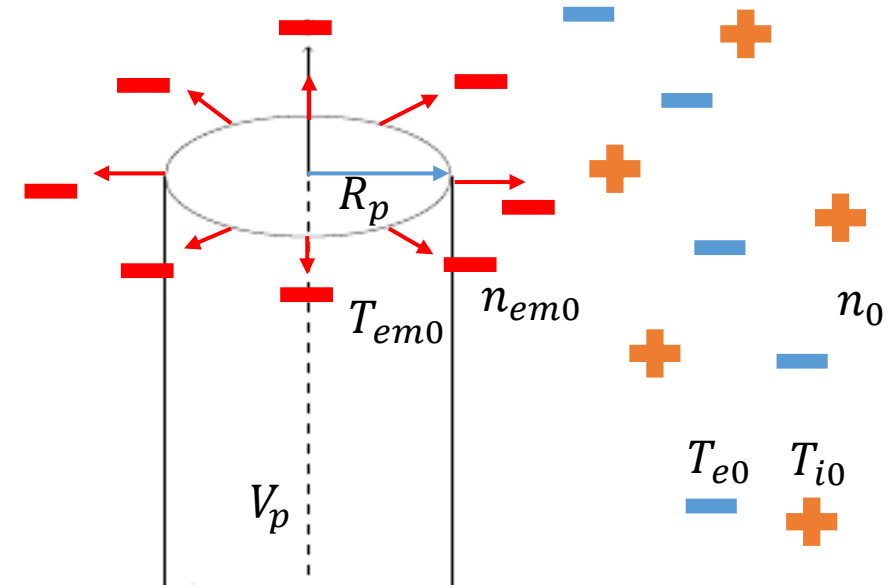
- Theoretical models on cylindrical emissive probes are useful for:
 - Plasma diagnostics
 - Electrodynamic tethers
 - Dusty plasma
- They also provide sheath structure and macroscopic quantities.



Introduction

Orbital Motion Theory

- Unmagnetized, collision-less and stationary plasma.
- Maxwellian plasma species, half-Maxwellian emitted electrons.
- No trapped particles.
- A Vlasov-Poisson solver was recently presented: X. Chen and G. Sanchez-Arriaga, “*Orbital motion theory and operational regimes for cylindrical emissive probes,*” *Physics of Plasmas* 24, 023504 (2017).



Introduction

- The distribution function (Collision-less plasma), transverse energy (Stationary conditions), and angular momentum (Cylindrical geometry) are all conserved.
- They are used to write the Vlasov-Poisson system as a single integro-differential equation.
- After discretization, it becomes a set of nonlinear algebraic equations.

$$\mathbf{F}(\boldsymbol{\phi}) \equiv \boldsymbol{\phi} - \mathbf{P}[\mathbf{V}[\boldsymbol{\phi}]] = 0$$

with $\boldsymbol{\phi}$ a vector with the values of the electrostatic potential at the mesh.

- A Newton method is implemented

$$\boldsymbol{\phi}_{i+1} = \boldsymbol{\phi}_i - \bar{\mathbf{J}}^{-1}|_{\boldsymbol{\phi}_i} \mathbf{F}(\boldsymbol{\phi}_i)$$

Introduction

- Article by Chen and Sanchez-Arriaga (2017)
 - Details of the Vlasov-Poisson solver were presented.
 - Achievements:
 - Computing the Current-Voltage (IV) characteristics of cylindrical emissive probes.
 - Identifying the operational regimes: Orbital Motion Limited (OML) and Space Charge Limited (SCL).
 - Limitations:
 - High computational cost due to Finite Difference scheme in the computation of the Jacobian in the Newton-Raphson method.
 - Deep parametric studies were not possible.

IV Curve Database

IV Curve database

- Improvements in the algorithm:
 - Jacobian matrix was computed analytically.
 - Computational cost was reduced by a factor of 80.
 - Implementation of parallel architecture.
 - Efficient selection of probe bias in the computation of IV curves (selecting points close to transition regimes of operation).

IV Curve database

- Characteristics of the database:
 - More than 15000 IV curves were computed for these parameters ranges:

$$-1000 \leq \phi_p \equiv \frac{eV_p}{k_B T_{e0}} \leq 1000$$

$$0 \leq \beta \equiv \frac{N_{em0}}{N_0} \leq 500$$

$$0.1 \leq r_p \equiv \frac{R_p}{\lambda_{De}} \leq 10$$

$$0.05 \leq \delta_i \equiv \frac{T_{i0}}{T_{e0}} \leq 3$$

$$\delta_p \equiv \frac{T_{em0}}{T_{e0}} = \text{linked to } \beta \text{ by Richardson Duchman law}$$

- Transition regimes and floating potential were identified.

I-V Curves

- For a given set of physical parameters $(\phi_p, \beta, \delta_p, \delta_i, r_p)$, the solver computes a potential profile.
- For $\mu_i = m_i/m_e$, i_α can be calculated:

$$i_\alpha = \frac{I_\alpha}{I_{th}}, \quad I_{th} = 2\pi R_p e N_0 \sqrt{\frac{k_B T_e}{2\pi m_e}}$$

$$j = i_e - i_{em} - i_i$$

● Electron OML Transition

■ Ion OML Transition

◆ SCL Transition

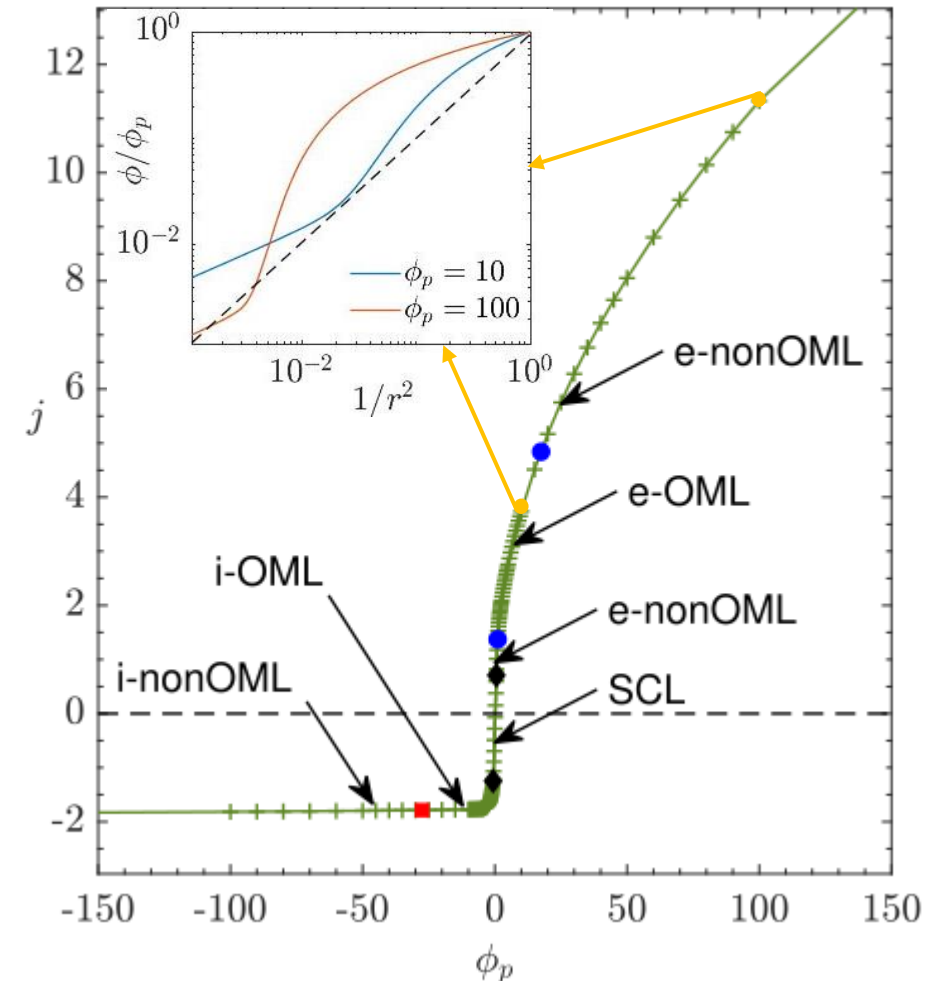


Fig.1: I-V characteristics of $\beta = 1.456$, $r_p = 1.1$, $\delta_i = 1$, $\delta_p = 0.361$ and $\mu_i = 29164$.

I-V Curves

- For a given set of physical parameters $(\phi_p, \beta, \delta_p, \delta_i, r_p)$, the solver computes a potential profile.
- For $\mu_i = m_i/m_e$, i_α can be calculated:

$$i_\alpha = \frac{I_\alpha}{I_{th}}, \quad I_{th} = 2\pi R_p e N_0 \sqrt{\frac{k_B T_e}{2\pi m_e}}$$

$$j = i_e - i_{em} - i_i$$

● Electron OML Transition

■ Ion OML Transition

◆ SCL Transition

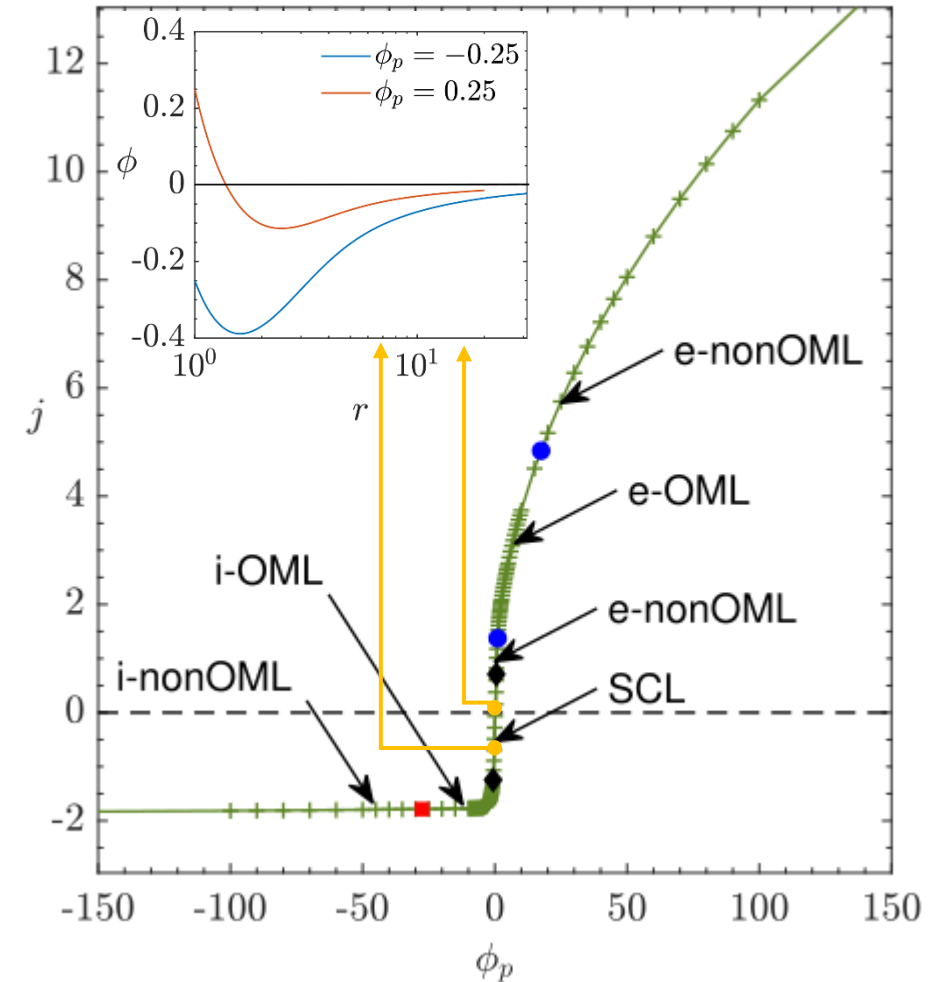


Fig.1: I-V characteristics of $\beta = 1.456$, $r_p = 1.1$, $\delta_i = 1$, $\delta_p = 0.361$ and $\mu_i = 29164$.

Numerical Results

Emission Level Variation

- Effect on the current & Space Charge Limit (SCL) region ($i_{em} < i_{RD}$).
- Operational regimes of emissive probe in ϕ_p vs. β plane.

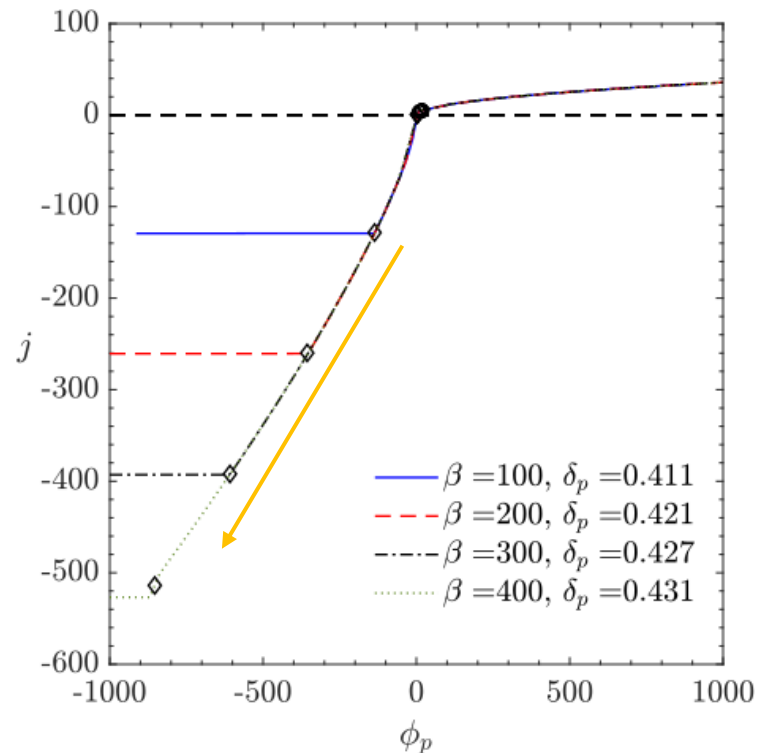


Fig.2: I-V characteristics of $r_p = 1.1$, $\delta_i = 1$ and different values of δ_p and β .

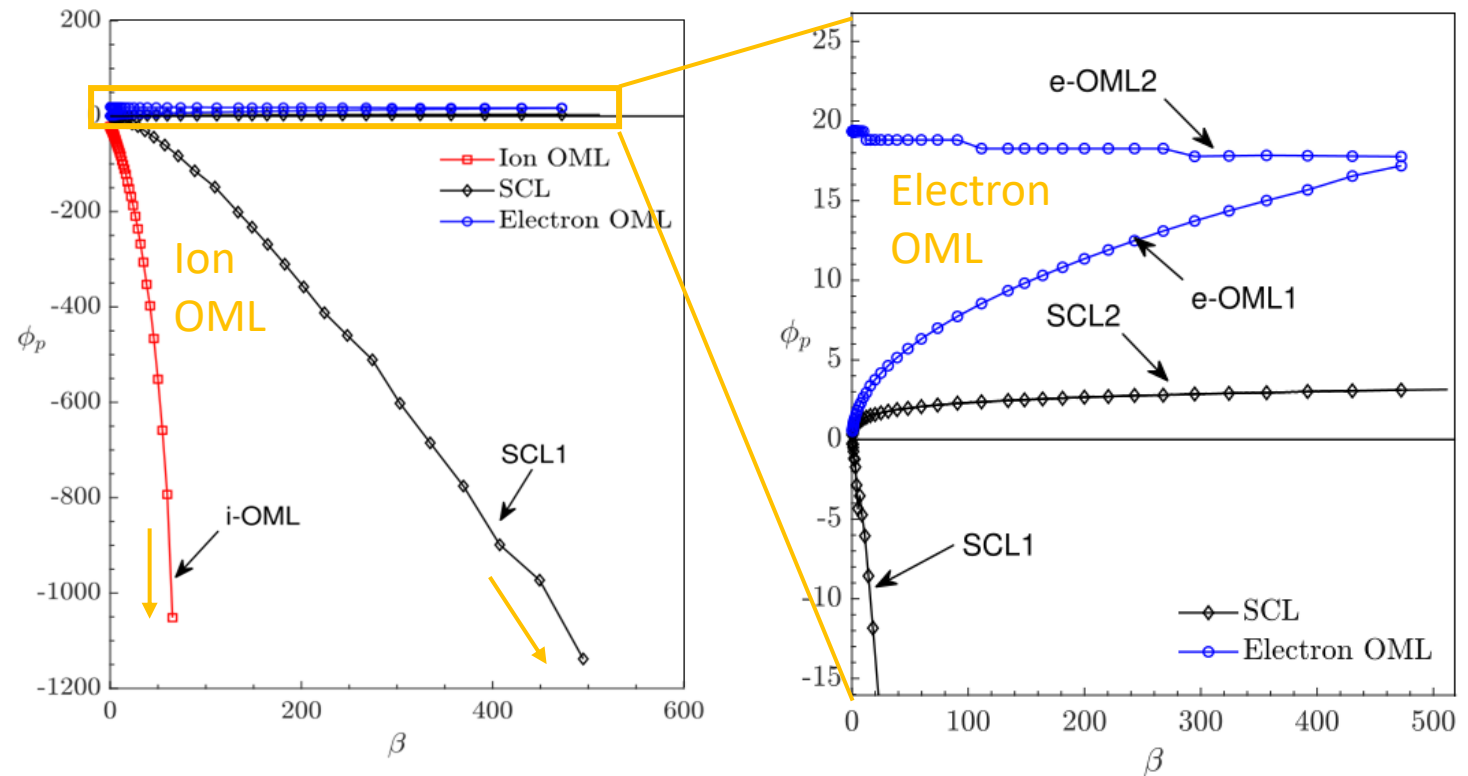


Fig.3: Ion OML, SCL and electron OML transition boundaries for $r_p = 1.1$ and $\delta_i = 1$.

Probe Radius Variation

- As r_p increases:

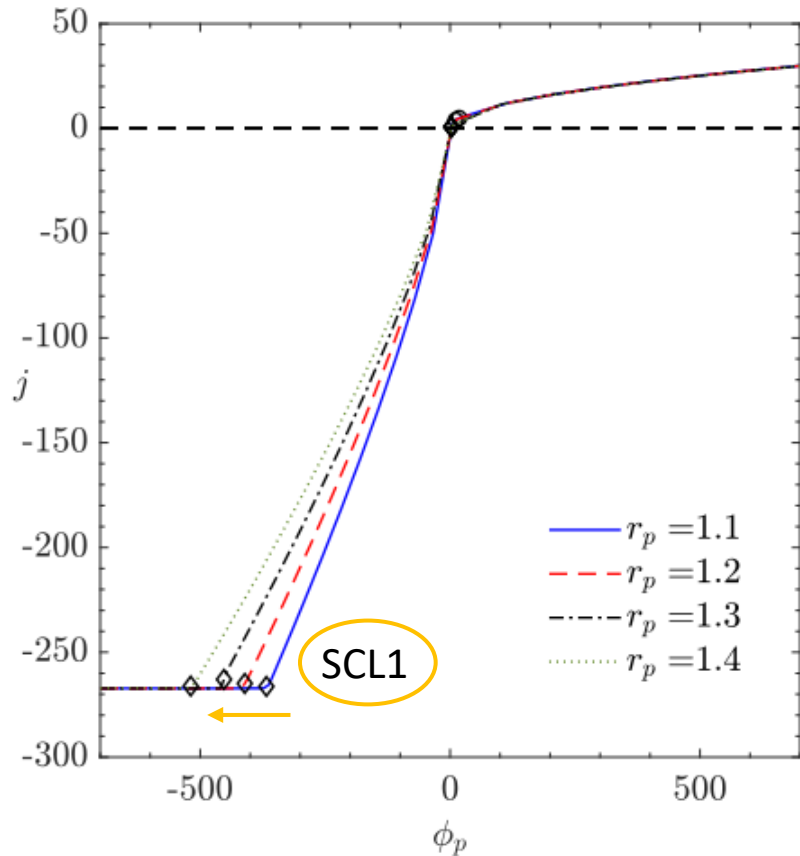


Fig.4: I-V curve of $\beta = 205.7$, $\delta_i = 1$ and $\delta_p = 0.421$ and different values of r_p .

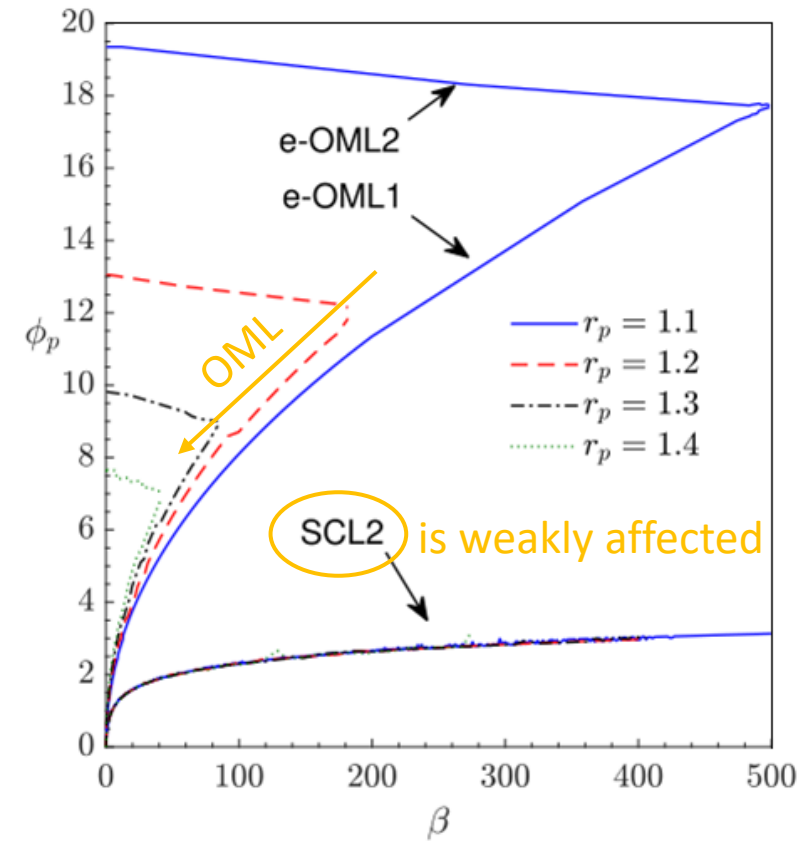
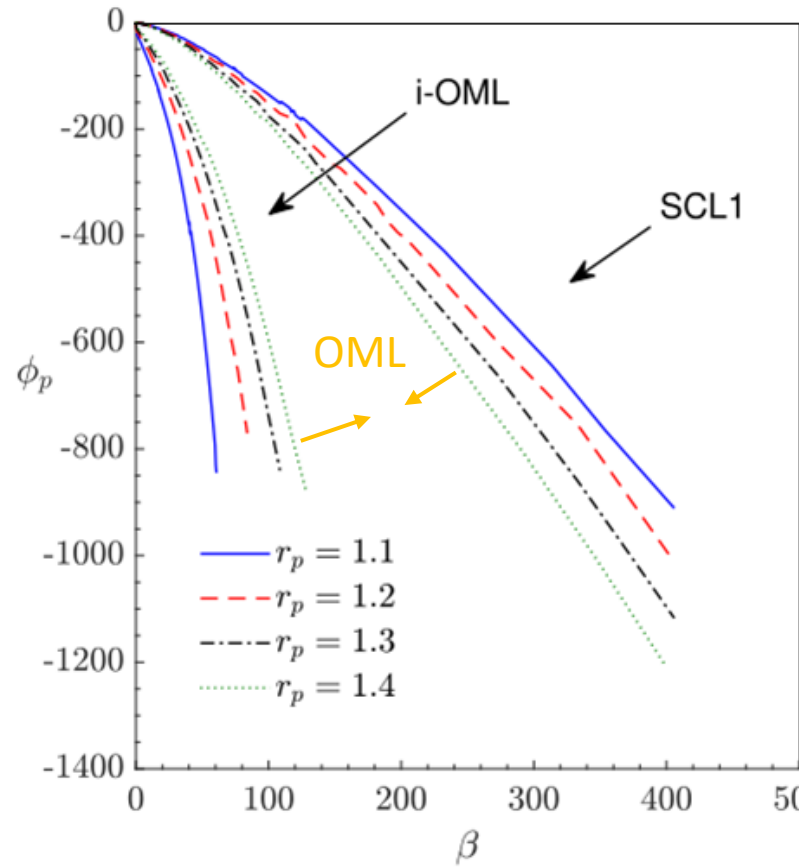


Fig.5: Ion OML, SCL and electron OML transition boundaries for $\delta_i = 1$ and different values of r_p .

Floating Potential Curve Fitting

- When $j = 0$ then $\phi_p = \phi_f$.
- Saturation has not been observed at high emission levels.
- Floating potential relation with emission level:

$$\phi_f = p_1(r_p) \log \beta + p_2(r_p)$$

- Probe radius affects weakly the floating potential.

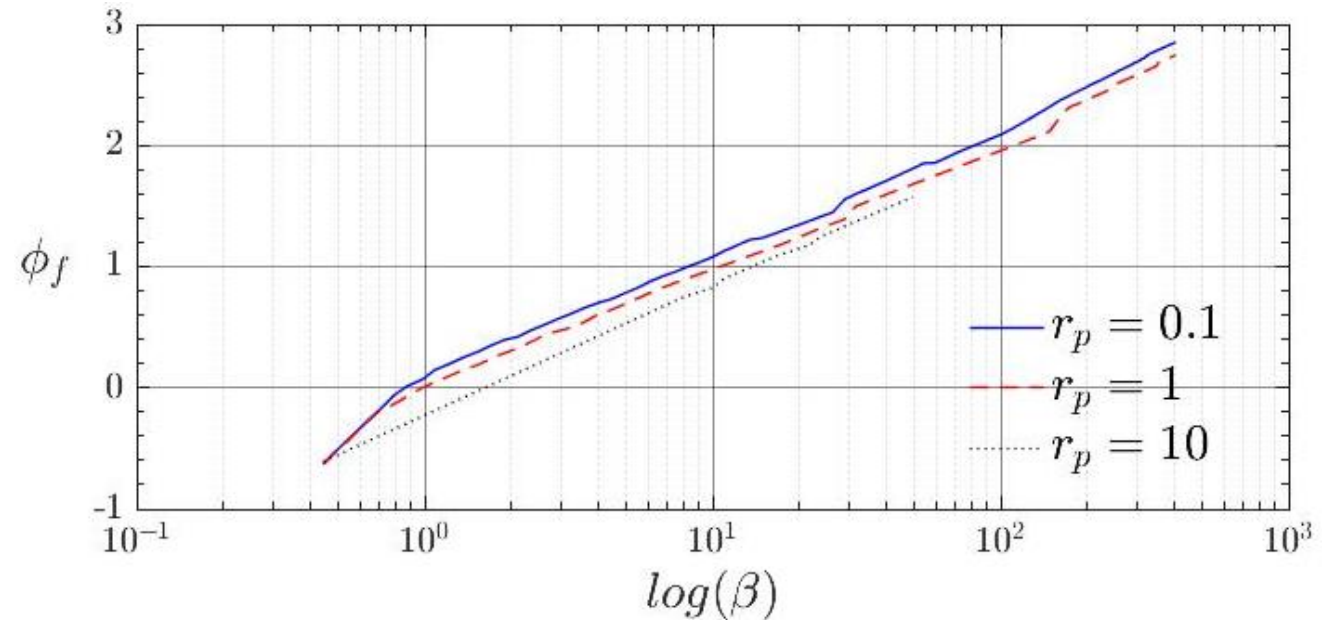


Fig.8: Floating potential versus emission level for $\delta_i = 1$ and different values of r_p .

Conclusions and Future Work

Conclusions and Future Work

- The 15000 IV curves and friendly software to extract the information will be soon available at www.etpack.eu
- Interested users will be able to
 - Plot IV curves.
 - Plot transition boundaries in parameter space.
 - Plot macroscopic quantities profiles (densities, potential, temperatures).
 - Plot distribution functions.
 - Construct fitting laws for interesting quantities (floating potential).
- More information will be available at:
S. Shahsavani, X. Chen, G. Sanchez-Arriaga, “*Current-Voltage characteristics of cylindrical emissive probes in collisionless Maxwellian plasmas at rest*”



Thank you for your attention!

Sadaf Shahsavani, Xin Chen, G. Sánchez-Arriaga

Universidad Carlos III de Madrid, Spain

APS-DPP 2020, 9-13 November